Staphylococcus aureus prophages are gatekeepers of lipid utilization to control membrane plasticity, bacterial fitness, and antibiotic adaptation

Byang Zhou,[a] Amit Pathania,[a] Deepak Pant,[a] David Halpern,[a] Philippe Gaudu,[a] Patrick Trieu-Cuot,[b] Alexandra Gruss,[a] and Karine Gloux,[a]#.

[a]Université Paris-Saclay, INRAE, AgroParisTech, Micalis Institute, Jouy en Josas, France,

[b]Institut Pasteur, Université Paris Cité, CNRS UMR 2001, Unité de Biologie des Bactéries Pathogènes à Gram-Positif, Paris, France.

Running Head: Prophages Control *S. aureus* Fitness in Lipids

Key words: triglycerides, diglycerides, sphingomyelins, fatty acids, fatty acid synthesis pathway (FASII), bacteriophages, Geh lipase, Hlb sphingomyelinase C, FakB1, FASII antibiotic.

#Adress correspondence to Karine Gloux, karine.gloux@inrae.fr

Word count for the abstract [246 words]

Word count for the text [3884 words]

Abstract

Lipids are essential components of bacterial membranes and phages are quasi-ubiquitous in bacteria. In the human pathogen *Staphylococcus aureus*, two common prophages ϕ13 and ϕ11.1 are preferentially integrated in lipase genes, and act as regulatory switches of respectively Geh, a triglyceride lipase, and Hlb, a sphingomyelinase. The factors driving selection for this prophage conservation in lipase genes and the impact on *S. aureus* fitness are not well understood. We report that prophage status of both ϕ13 and ϕ11.1 affect membrane phospholipid composition and bacterial growth in serum. They vary the extent to which toxic C18:2, released from Geh activity on triglycerides, are incorporated in bacterial membranes. Hlb and Geh lipases lead respectively to palmitic acid C16 and linoleic acid C18:2, which compete for binding to fatty acid kinase subunit FakB1. When both lipases are active, interference from C16 decreases C18:2 incorporation *via* FakB1 and reduces fatty acid synthesis (FASII)-mediated elongation. In the presence of FASII inhibitor AFN-1252, *S. aureus* relies on exogenous fatty acids, and adapts faster when Hlb is intact (ϕ13 absent), but slower when Hlb is inhibited. Faster adaptation correlates with less incorporation of C18:2. These findings contribute to explaining the selective advantage of Hlb-conversion by ϕ13 as a means of increasing membrane plasticity and *S. aureus* adaptation to environmental lipids. They also reveal an effect of ϕ13 status on anti-FASII adaptation. Prophage status and host-specific lipid environments may be important for accurate prediction of *S. aureus* infection risk and efficacy of new therapeutics.

Importance

Staphylococcus aureus is a major cause of untreatable human bacterial infections and its lipases are crucial for virulence and immune response escape. Prophages inserted in these lipase-encoding genes able to reversibly switch their activities are common in *S. aureus,* but the selective benefits of their maintenance is little understood. We demonstrate that two prophages, inserted in triglyceride and sphingomyelin lipase genes, interactively modulate fatty acid incorporation into bacterial membranes. The presence or absence of these prophages determine how *S. aureus* adapts to lipid environments, by affecting membrane plasticity, bacterial fitness, and adaptation to an antibiotic inhibiting fatty acid synthesis. Our findings highlight the importance of assessing *S. aureus* prophages and host lipid environments when evaluating infection risk and therapy efficacy.

Introduction

Environmental lipids comprise an integral, but often overlooked, aspect of bacterial pathogenesis. Lipids can be crucial for bacterial fitness and front-line players in modulating interactions with the host (1-4). Lipids range in structure from simple short hydrocarbon chains to complex molecules, including triglycerides (TG), phospholipids (PLs), and esterified sterols. Fatty acids (FAs), the basic constituents of complex lipids, vary in chain length, side chains, and number and position of double bonds. A vast array of bacteria scavenges FAs, which are incorporated in membranes (5-10). The quasi-ubiquity of FA scavenging suggests a great potential of the host lipid environment to modulate invading pathogen behavior. The environmental lipid composition depends on human genetics and diet, which correlate to risk of infection (2, 3, 11, 12). *Staphylococcus* aureus, a major human pathogen, incorporates exogenous FAs, such as those present in plasma lipids (6, 13). The incorporation involves a FakAB system

including the FakA FA kinase and the FakB1 and FakB2 FA binding proteins conferring preference for saturated and unsaturated FAs, respectively (14-16). While *S. aureus* lacks unsaturated fatty acid synthesis and desaturase functions (17), incorporation of monounsaturated fatty acids (UFAs) and polyunsaturated FAs (PUFAs) has crucial effects on bacterial membrane functions and interactions with the host (18-22).

Prophages are potent factors of virulence, as reported in *S. aureus* (23). Remarkably, two commonly found *S. aureus* prophages, ϕ11.1 and ϕ13, are inserted in *geh* and *hlb* genes encoding the lipases Geh (glycerol ester hydrolase; EC 3.1.1.3) and Hlb (neutral sphingomyelinase C, also called hemolysin B; EC 3.1.4.12), respectively (24, 25) (Fig. 1A). About 15% of *S. aureus* isolates carry ϕ11.1 in *geh* (ϕ11 lysogen); remarkably over 90% of human clinical isolates carry ϕ13 in *hlb* (ϕ13 lysogen) (1, 26). ϕ13 prophage was quasi-absent in livestock isolates but can be acquired from human strains in the presence of biocides (27). ϕ11.1 and ϕ13 prophage excision is induced by environmental signals (such as biocides or reactive oxygen species), leading to reactivation of Geh and Hlb activities with consequent impacts on bacterial virulence (1, 27-32). They are also pseudolysogenic prophages that can be maintained in episomic form and reintegrate the bacterial chromosome (33). To date, the driving force for maintaining ϕ13 in the *hlb* gene in humans is unknown and consequences of truncation of these lipases on bacterial lipid metabolism and physiology have been little explored (13). Geh is one of the two *S. aureus* TG lipases and is differentiated by cleavage preferences on the glycerol backbone (Fig. 1B). Whereas most TG lipases prefer position 1, Geh cleaves in both positions (34, 35). The role of this extended cleavage property in *S. aureus* physiology remains to be elucidated. Here we show that these two widespread prophages interactively affect membrane PL composition and bacterial growth in response to host lipid sources of C18:2, which is toxic (36). Differential FAs released from Geh and Hlb activities, constitute a basis for phage interference. The unexpected competition

between FAs issued from TG and sphingomyelin hydrolysis for the FA binding protein FakB1 is identified as a key control point. Furthermore, ϕ13 lysogeny leads to impaired efficiency of an antibiotic targeting the fatty acid synthesis pathway (anti-FASII). We propose a model for the roles of ϕ13 and ϕ11.1 prophages and *fakB1* as gatekeepers of lipid utilization in *S. aureus*. Our findings underline the importance of environmental lipids and prophages as regulatory switches in *S. aureus* fitness and anti-FASII adaptation.

Results

ϕ13 lysogeny increases C18:2 incorporation from serum into *S. aureus* phospholipids. We analyzed FAs profiles from two isogenic Newman strains (WT and Δϕ13), which differ by the presence of ϕ13 prophage (21). The ϕ13-lysogenized WT and the isogenic Δϕ13 strain showed identical FAs profiles in control BHI medium, indicating that FASII-synthesis was unaffected by ϕ13 (Fig. S1). In contrast, addition of 10% mouse serum, that has high PUFA linoleic acid (C18:2) level, distinguished the two strains by their incorporation of C18:2. The proportion of C18:2 was two-fold higher in the ϕ13-lysogen than in the strain deprived of ϕ13 (respectively 13 ± 1% and 6 ± 1%, Fig. 2A). These results suggested an unexpected link between the ϕ13 lysogenic status and the incorporation of serum-derived C18:2.

The impact of trilinolein on *S. aureus* fitness and phospholipids is increased in the absence of ϕ11 prophages and depends on ϕ13 status. TGs are major PUFA reservoirs in serum. Trilinolein (TNL), a TG comprising three C18:2 moieties, can be naturally present in diet and human fluids, and is hydrolyzed by Geh lipase. However, ϕ11.1, one of three ϕ11-type prophages in the Newman strain, interrupts Geh (Fig. 1A). We used TNL as substrate to determine if ϕ13 impacts incorporation of TG-derived C18:2, and whether ϕ11.1 affects this process. For this, we analyzed

FAs profiles of isogenic Newman strains lysogenized or not with ϕ11 prophages including ϕ11.1 (see Materials and methods) and ϕ13 (21). In BHI medium, the ϕ11 status had no detectable effect on endogenously synthesized FAs (Fig. S1). In contrast, TNL addition led to marked differences in *S. aureus* FAs profiles and growth. The ϕ11 lysogens showed less TNL-derived C18:2 incorporation and improved growth rate compared to the non-ϕ11 lysogens (Fig. 2B). This result is in accordance with C18:2 toxicity on *S. aureus* (36). Strikingly, ϕ11 lysogeny correlated with a quasi-total inhibition of C18:2 elongation by FASII (Fig. 2B). In the ϕ11 lysogen background, ϕ13 lysogeny allowed higher C18:2 incorporation from TNL (11 ± 1% in the WT double lysogen *versus* 4 ± 0.5% in Δϕ13 strain). In contrast, in the absence of ϕ11 prophages, total C18:2 incorporation was not impacted by the ϕ13 status (28 ± 4% in Δϕ11 *versus* 28 ± 1% in Δϕ11Δϕ13 strain, Fig. 2B). Nevertheless, elongation of both 18:2 and C20:2 was increased in the presence of ϕ13 (C18:2, from 50 to 70% and C20:2, from 14 to 28%). These observations point to impacts of ϕ13 and ϕ11 status on bacterial fitness and C18:2 incorporation. They also show that ϕ13 somehow determines the extent of C18:2 elongation.

***geh* interruption by ϕ11.1 reduces C18:2 incorporation.** ϕ11.1, one of the three ϕ11 prophages present in the Newman strain, interrupts *geh* gene encoding Geh which hydrolyzes TGs including TNL (37)(Fig. 1B). We asked whether the observed effect of ϕ11 lysogeny on TNL-derived C18:2 incorporation was due to *geh* interruption by ϕ11.1. We used *S. aureus* USA300, which lacks ϕ11.1 (*geh* is intact), and its isogenic *geh::tn* mutant, encoding a C-terminal truncated Geh similar to that generated by ϕ11 insertion (transposon at amino acid [aa] position 517 compared to ϕ11 insertion at position 643, for a full length protein of 690 aa). Incorporation of TNL-derived C18:2 was significantly lower in the *geh*::tn mutant compared to the WT (Fig. 3A). Upon treatment with orlistat, a Geh inhibitor (38), incorporation of TNL-derived C18:2 was decreased (Fig. 3A). The remaining 18:2 incorporation in the ϕ11 lysogens may indicate some conserved activity in the

truncated Geh, or TNL hydrolysis by other lipases. These results indicate that the Geh state, rather than an intrinsic property of ϕ11 prophages, determines *S. aureus* capacity to incorporate TNL-derived C18:2.

C18:2 is efficiently incorporated from 1,3-diglyceride. In contrast to most lipases, Geh cleaves in both positions on the glycerol and can release higher level of 1,3-dilinoleoylglycerol (1.3DG) from TNL (34, 35) (Fig. 1B). We questioned if this specificity can affect the incorporation and toxicity of PUFA released from TGs. We examined C18:2 incorporation in the presence of 1.2DG or 1.3DG in the WT strain and the Δϕ11, Δϕ13 and Δϕ11Δϕ13 Newman isogenic mutants. Addition of 10 µM 1.2DG had no effect on growth (Fig. S2) and led to very low-level C18:2 incorporation whatever the prophage status (Fig. 3A). In contrast 10 µM 1.3DG led to a high incorporation of C18:2 in the four strains (Fig. 3A) and a high toxicity in the *geh*$^{+}$, *hlb*$^{-}$ strain (Δϕ11 Newman, Fig. S2). 1.3DG, a TG hydrolysis product particularly attributed to Geh activity, leads therefore to high incorporation of C18:2 and also to high toxicity depending on ϕ11ϕ13 status.

***hlb* decreases 1.3DG toxicity and FASII activity, and increases C16 incorporation.** To determine if *hlb* affects 1.3DG-derived C18:2 incorporation and elongation, we complemented the USA300 *hlb::tn* mutant with a plasmid carrying an *hlb* gene and compared growth in the presence of serum and without or with 10 µM 1.3DG. The strain carrying p*hlb* grew more slowly than the control plasmid strain in the presence of serum (Fig. 4). *hlb* protects *S. aureus* from serum compounds. While *hlb* complementation had low protecting effect against 1.3DG toxicity, it restored growth in the presence of activated sphingomyelin, a state needed for Hlb activity (see Material and methods) (Fig. 4). These results indicate that Hlb contributes to protecting *S. aureus* from 1.3-derived C18:2 toxicity. In second step, we questioned for a potential release of sphingomyelin-derived FA that may interfere with C18:2 incorporation. Serum sphingomyelins

are dominant circulating Hlb substrates that contain mainly C16 as FA moieties (39, 40) and the *hlb* complementation increased C16 incorporation from serum even without added activated sphingomyelin (Fig. 4). Hlb activity on serum is therefore sufficient to liberate sphingomyelin derived-C16 and modulate PL composition. Interestingly added sphingomyelin had no effect on C16 incorporation in PLs but it decreased elongation of both C16 and C18:2 specifically in the *hlb* complemented strain (Fig. S3), suggesting protecting mechanism independent of C16 contribution to PLs. These results further indicate that Hlb activity is a determining factor in ϕ13 status impacts on 1.3DG-derived C18:2 toxicity and elongation.

Incorporation of 1.3DG-derived C18:2 requires *fakB1* kinase gene and is competitively inhibited by C16. FakA kinase is essential for incorporation from all FAs (14) but FakAB system has substrate selectivity conferred by FakB1 and FakB2 for saturated and unsaturated FAs, respectively (14-16). These expected phenotypes were confirmed in USA300 derivative *fakA*, *fakB1*, and *fakB2* mutants when medium was supplemented with free FAs (Fig. S4). The role of FakB2 in free PUFA incorporation was also confirmed using free C18:2 (Fig. S5)(16). We then challenged USA300 derivative *fakA*, *fakB1*, and *fakB2* mutants with TNL. The *fakA* mutant did not incorporate TNL-derived C18:2 (Fig. S6) but *fakB1* and *fakB2* mutants unexpectedly failed to show selectivity; both mutants displayed the same capacity to incorporate C18:2 from this TG (Fig. S7). Thus, while free C18:2 incorporation was FakB2-dependent (Fig. S5), incorporation of TNL-derived C18:2 was permissive and can use both acyl binding proteins.

The acyl position effect on FA incorporation (Fig. 1B), led us to examine incorporation of 1.2DG and 1.3DG in the *fakA*, *fakB1*, and *fakB2* backgrounds. Incorporation of 1.2DG-derived C18:2 was greatly decreased in the *fakB2* mutant (Fig. S8), in accordance with the reported FakB2 binding phenotype (14-16). In contrast, incorporation of 1.3DG-derived C18:2 was higher in the *fakB2*

mutant than in the *fakB1* mutant (20 ± 7% versus 13 ± 3%; incorporation in the USA300 WT strain being 31 ± 5%, Fig. 5A). Furthermore, growth of the *fakB1* mutant was strongly impaired by 1.3DG compared to the WT strain (Fig. 5B). These results demonstrate that FakB1 is important for 1.3DG-derived C18:2 incorporation and suggest that its binding may prevent free C18:2 toxicity.

The unexpected role of FakB1 in the incorporation of TNL- and 1.3DG-derived C18:2 (Fig. S7, Fig. 5A) and the increased C16 incorporation by the *hlb* complementation led us to hypothesize that C16 can compete with 1.3-derived C18:2 for FakB1. To test this, C16 was added in experiments discussed above. In the USA300 WT and *fakB1* strains, addition of free C16 led to only a slight decrease in C18:2 incorporation from either TNL or 1.3DG (Fig. S7, Fig 5A). In contrast, in the *fakB2* mutant (when only FakB1 is available), C16 addition led to a quasi-total arrest of C18:2 incorporation from either TNL- or 1.3DG- derived C18:2 (Fig. S7, Fig 5A). Interestingly, in this mutant, FakB1 protects growth from the 1.3DG toxicity and this effect is reversed in the presence of C16 (Fig. 5B). This result suggests that 1.3DG-derived C18:2 binds to FakB1 and that competition with the preferred substrate C16 releases the toxic C18:2.

To confirm the direct role of *fakB1* in 1.3DG-derived C18:2, we used the RN450 strain, which is cured of phage lysogens but carries a natural *fakB1* in-frame deletion (483-bp within the 867-bp functional gene, Fig. S9). A derivative strain called RN450-R is repaired for *fakB1*. The 1.3DG-derived C18:2 is more efficiently incorporated by the RN450-R repaired strain than by the *fakB1* deficient RN450 strain (35 ± 3% and 27± 3% respectively, Fig. 6A). Whereas C16 had no effect on the incorporation of 1.3DG-derived C18:2 in the RN450 strain, it strongly inhibited this incorporation in the R450-R strain (80 ± 10% decreased, Fig. 6A). The growth in the presence of 1.3DG was better in *fakB1* repaired strain than in the WT (Fig. 6B). In contrast to the USA300 *fakb2* mutant (Fig. 5B and Fig. S7), the growth of RN450-R was not affected by C16. This may

reflect unrepresentative strain specificity due to atypical mutations occurring after prophage curing (41). However, these observations identified FakB1 binding as the unconventional preferred pathway for incorporation of 1.3DG-derived C18:2 into PLs. The saturated FA C16 competes for FakB1 and is a key determinant for 1.3DG-derived C18:2 incorporation and may also affect growth.

ϕ13 lysogeny and GW4869, an inhibitor of Hlb activity, delay *S. aureus* adaptation to AFN-1252, an anti-FASII. We showed previously that *S. aureus* can overcome inhibition by anti-FASII only in the presence of serum, by incorporating exogenous FAs (6). This study shows that ϕ13 lysogeny affects incorporation of FAs from both sphingomyelins and TGs, which are lipids present in serum. We therefore considered that ϕ13 lysogenic status might impact *S. aureus a*daptation to anti-FASII. This was studied using ϕ13 lysogen and non-lysogen Newman strains and the antibiotic AFN-1252 which targets the FASII enoyl reductase enzyme FabI (42). Serum-supplemented BHI medium was enriched with 1.3DG likely released in the host by the active Geh (1) (Fig. 2). The absence of ϕ13 resulted in markedly faster *S. aureus* outgrowth in AFN-1252-containing medium (Fig. 7A). To confirm the potential role of Hlb, we used GW4869, a specific inhibitor of the sphingomyelinase lipid activation (43, 44)(see material and methods). In the absence of AFN-1252, 50 µM GW4869 had negligible effects on growth of both ϕ13 and Δϕ13 strains (Fig. S10). In the presence of AFN-12, GW4869 did not significantly change the latency period before outgrowth of the ϕ13 lysogen, in accordance with an absence of Hlb activity in this strain. In contrast, GW4869 addition in the presence of AFN-1252 prolonged the latency period of the Δϕ13 strain. We observed that, GW4869 supplementation highly increased C18:2 incorporation in the Δϕ13 strain, even if 1.3DG is not added (Fig. 7B). These observations indicate that ϕ13 prophage affects adaptation to the anti-FASII and that Hlb lipase activity promotes outgrowth.

They are also consistent with a competition between FAs, released from serum by Hlb activity, and toxic C18:2 incorporation. Hlb activity may therefore facilitate adaptation to anti-FASII.

Discussion

S. aureus responses to environmental lipids are modulated by two common prophages, ϕ11.1 and ϕ13, whose excision/integration status determines activities of the TG lipase Geh and the sphingomyelinase Hlb, respectively (1, 28, 33). The present work reveals expanded roles for these prophages in lipid utilization, leading to increased membrane plasticity and growth adaptation. We first observed that ϕ13 lysogeny increases C18:2 incorporation from serum and we further investigated the potential connection with hydrolysis of TG, a main source of C18:2 in serum. Our work revealed that ϕ13 and ϕ11.1 status affects bacterial phospholipid variability and fitness due to the Geh and Hlb activities, which release FAs competing for FakB1. A mechanistic model schematizing the roles of ϕ11.1, ϕ13 and *fakB1* as gatekeepers of phospholipid variability and TG-derived C18:2 toxicity is proposed (Fig. 8A). Briefly, three major factors determine how ϕ13 status affects bacterial fitness: the lipid environment, particularly TGs and sphingomyelins and their respective content in PUFAs such as C18:2 and saturated FAs such as C16; the presence or not of ϕ11.1 in *geh*, which modulates liberation of toxic diglycerides; and the FA kinase cofactor FakB1, which controls competitive entry of the released 1.3 diglyceride *vs* saturated FAs. The different combinations of ϕ11.1/ϕ13 status, which vary according to strains and stress-induced excision, determine PL composition possibilities (with respect to PUFA, SFAs and elongated FAs) and growth response to the lipid environment.

The present work further shows that ϕ13 lysogeny, which is prevalent among clinical isolates (26), delays adaptation of a *geh*$^{+}$ ϕ13 $^{+}$ Newman strain to FASII antibiotic. In agreement with the above model, treatment by an Hlb inhibitor also slows adaptation to the anti-FASII and increases serum-derived C18:2 incorporation by the isogenic Δϕ13 (Hlb^{+}) strain. A proposed model schematizes how ϕ13 status affects *S. aureus* adaptation to anti-FASII (Fig 8B). In this model, the toxic effects of C18:2 incorporation are exacerbated by FASII inhibition and the consequent exogenous FAs requirement, such that outgrowth and adaptation are delayed.

The results of this study offer new insights into the roles of lipase-converting prophages during infection of the lipid-rich host. The dual states of ϕ11.1 and ϕ13, as prophage and episomic forms (33), imply rapid and reversible regulation of Geh and Hlb activities to redesign bacterial membranes and adapt to toxic lipids. The composition and levels of TGs and sphingomyelins vary in humans according to genetic makeup, the state of health, and diet, all of which may be risk determinants during infection (40, 45-49). TGs are reservoirs of long chain UFAs, which alter bacterial membrane functions and host interactions (6, 18, 19, 22, 50). Cholesterol esters, which are common serum lipids, were also recently reported as Geh substrates (18). The effects of ϕ13 on FA incorporation from these lipids needs to be studied. ϕ 13 carriage is energetically costly to bacteria: we suggest that its conservation at the *hlb* insertion site may contribute to optimizing human FA utilization and limiting FA toxicity. These results offer perspectives on the rationale for the very high ϕ13 frequency in clinical isolates (26).

In conclusion, ϕ13 and ϕ11.1 are interactive regulators of *S. aureus* membrane PL composition that modulate bacterial responses to environmental lipids present in the host. The capacity to control lipase activities makes these prophages active gatekeepers of FA toxicity, membrane plasticity and consequently bacterial fitness. These findings demonstrate the need to assess

prophage status when developing antimicrobial strategies against *S. aureus* infection. Further investigation of lipase-converting prophages in response to diverse human lipidomes may contribute to understanding the risk of developing severe visceral infections and to resist to antimicrobial treatment.

Materials and methods

Bacterial strains. *S. aureus* Newman, USA300 FPR3757 JE2 (called here USA300), and NCTC 8325 derivative strains RN450 and RN450-R, were used in this study. Isogenic Newman strains differentiated by the presence of prophages, WT, TB3 (Δϕ11), TB1 (Δϕ13) and TB4 (Δϕ11,Δϕ13), were provided by the Schneewind laboratory (Department of Microbiology, University of Chicago). Newman strain has 4 prophages which are from Siphoviridae family: ϕ11.1, ϕ11.2 and ϕ11.3 from Sfi 11/Sa6 subfamily and ϕ13 from Sfi 21/Sa3 subfamily (25). In the Δϕ11 strains used in this study, the three ϕ11 prophages were absent. Methicillin-resistant USA300 and the Nebraska library of transposon insertions (University of Nebraska Medical Center) were generously supplied by BEI resources (51). The library USA300 derivatives used in this work contained insertions in the following genes: SAUSA300_0320 (*geh*), SAUSA300_1973 (*hlb*), SAUSA300_1119 (*fakA*), SAUSA300_0733 (*fakB1*), SAUSA300_1318 (*fakB2*); all mutants were verified by PCR. RN450 is a phage-free derivative of the NCTC 8325 strain (52). It was repaired for a natural *fakB1* deletion as described for another strain (53).

Construction of *hlb* complemented strain. A PCR fragment, containing *hlb* promoter and open reading frame SACOL_RS10470 (-355 from ATG start codon and +40 after TAG stop codon) from the *S. aureus* subsp. *aureus* COL, was cloned in EcoRI and SmaI sites of modified pAW8 (54). The

primers pairs used for the PCR are 5'-TTGCCGGAATTCTGCAACTTAATTATAGCCAGACTTTC-3' and 5'-CATCAACCCGGGCGTCCTTTTAGAACGAAGCAAG-3'. Genomic co-ordinates of the 1388 bp cloned segment are 2063371-2064758, as present on plasmid p*hlb* further used for complementation experiment.

Construction of *fakB1*-repaired strain. *S. aureus* RN450 (also designated as 8325-4), as the entire NCTC 8325 lineage, displays a 483-bp deletion in the *fakB1* gene, removing 56% of the 867-bp functional gene (Fig. S9). To repair this deletion, a 1,939-bp DNA fragment containing a functional *fakB1* was amplified as described for other NCTC 8325 derivatives (53). The *fakB1*-repaired strain is designated as RN450-R.

Growth media and conditions. Brain heart infusion (BHI) was the base medium for *S. aureus* cultures. Cultures were grown aerobically at 37°C and the starting OD_{600nm} was 0.02 from a preculture at OD_{600nm} between 1 and 4 depending on the experiment. Growth were presented as OD_{600nm} /h for short times required for determination of FAs profiles and C18:2 incorporation. Mouse serum (Clinisciences, France) was added at 10% final concentration. Stocks of trilinolein (TNL, 50 mM), 1,2-dilinoleoylglycerol (1.2DG, 50 mM), 1,3-dilinoleoylglycerol (1.3DG, 50 mM), palmitic acid (C16, 100 mM) (Larodan Fine Chemicals, Sweden), orlistat (38 mM, MedChemExpress, France), and the anti-FabI antibiotic AFN-1252 (1 mg/ml, MedChemExpress, France) were prepared in DMSO. To follow *S. aureus* adaptation to AFN-1252, bacteria were pre-cultured for 4 hours in BHI medium containing 10% mouse serum (Eurobio, France) and inoculated at OD_{600nm} 0.02 in the same medium containing 0.5 µg/ml AFN-1252. Cultures were performed in 96-well microtiter plates for 17 h at 37°C in a microplate Spark spectrophotometer (Tecan) and OD_{600nm} was measured every 20 min.

Substrate, inducer and inhibitor of sphingomyelinase activity. Sphingomyelin was from chicken egg yolk (Sigma-Aldrich; St. Louis, MO) and prepared as 50 mg/ml stock solution in chloroform/methanol (1:1)**.** Hlb sphingomyelinase belongs to the neutral sphingomyelinase family, which activity requires a lipid-dependent activation by phosphatidylserine. Phosphatidylserine (60 mM, bovine brain, Na salt, Larodan Sweden) was supplied in chloroform. GW4869 is an inhibitor specific of the universal conserved domain involved in such lipid-activation (43, 44). GW4869 (1.7 mM, Selleckchem.com) was prepared in DMSO.

Determination of *S. aureus* fatty acid profiles. FAs profiles were performed as described (7). Culture aliquots were routinely taken under exponential growth at low OD_{600nm} (between 1 and 4) and condition of optimum concentration of C18:2 donor in the culture. After sample preparation (7), analyses were performed in a split-splitless injection mode on an AutoSystem XL Gas Chromatograph (Perkin-Elmer) equipped with a ZB-Wax capillary column (30 m x 0.25 mm x 0.25 mm; Phenomenex, France). Data were recorded and analyzed by TotalChrom Workstation (Perkin-Elmer). FAs peaks were detected between 12 and 40 min of elution, and identified by comparing to retention times of purified esterified FA standards (Mixture ME100, Larodan, Sweden). Results are shown as representative gas chromatograph profiles, or as percent of specific FA as calculated from their proportions compared to total peak areas (TotalChrom Workstation; Perkin Elmer).

Statistics analysis. Graphs were prepared using Microsoft Excel software. Means and standard deviations are presented for culture growth (OD_{600nm} or OD_{600nm}/h) and percentages of FA or of FA elongation. Statistical significance was determined by unpaired, nonparametric Mann Whitney tests, as recommended for small sample sizes.

Acknowledgments: We gratefully acknowledge funding from the following French granting agencies: French Agence Nationale de la Recherche (StaphEscape project ANR-16-CE15-0013), and the Fondation pour la Recherche Medicale (DBF20161136769).

We thank Myriam Gominet (Institut Pasteur) for the construction of the *S. aureus* RN450 *fakB1*-repaired strain. We are grateful to members of the MicrobAdapt team for stimulating discussion of this work.

References

1. Chen X, Alonzo F, 3rd. 2019. Bacterial lipolysis of immune-activating ligands promotes evasion of innate defenses. Proc Natl Acad Sci USA 116:3764-3773.
2. Sun H, Zhang X, Shi W, Fang B. 2019. Association of soft tissue infection in the extremity with glucose and lipid metabolism and inflammatory factors. Exp Ther Med 17:2535-2540.
3. Trinder M, Boyd JH, Brunham LR. 2019. Molecular regulation of plasma lipid levels during systemic inflammation and sepsis. Curr Opin Lipidol 30:108-116.
4. Gajenthra Kumar N, Contaifer D, Jr., Baker PR, Ekroos K, Jefferson KK, Wijesinghe DS. 2018. Untargeted lipidomic analysis to broadly characterize the effects of pathogenic and non-pathogenic staphylococci on mammalian lipids. PLoS One 13:e0206606.
5. Gloux K, Guillemet M, Soler C, Morvan C, Halpern D, Pourcel C, Vu Thien H, Lamberet G, Gruss A. 2017. Clinical relevance of type II fatty acid synthesis bypass in *Staphylococcus aureus*. Antimicrob Agents Chemother. 61(5), e02515-16.
6. Kenanian G, Morvan C, Weckel A, Pathania A, Anba-Mondoloni J, Halpern D, Gaillard M, Solgadi A, Dupont L, Henry C, Poyart C, Fouet A, Lamberet G, Gloux K, Gruss A. 2019. Permissive fatty acid incorporation promotes staphylococcal adaptation to FASII antibiotics in host environments. Cell Rep 29:3974-3982 e4.
7. Morvan C, Halpern D, Kenanian G, Hays C, Anba-Mondoloni J, Brinster S, Kennedy S, Trieu-Cuot P, Poyart C, Lamberet G, Gloux K, Gruss A. 2016. Environmental fatty acids enable emergence of infectious *Staphylococcus aureus* resistant to FASII-targeted antimicrobials. Nat Commun 7:12944.
8. Morvan C, Halpern D, Kenanian G, Pathania A, Anba-Mondoloni J, Lamberet G, Gruss A, Gloux K. 2017. The *Staphylococcus aureus* FASII bypass escape route from FASII inhibitors. Biochimie 141:40-46.
9. Brinster S, Lamberet G, Staels B, Trieu-Cuot P, Gruss A, Poyart C. 2009. Type II fatty acid synthesis is not a suitable antibiotic target for Gram-positive pathogens. Nature 458:83-6.
10. Hays C, Lambert C, Brinster S, Lamberet G, du Merle L, Gloux K, Gruss A, Poyart C, Fouet A. 2021. Type II fatty acid synthesis pathway and cyclopropane ring formation are dispensable during *Enterococcus faecalis* systemic infection. J Bacteriol 203:e0022121.
11. Feingold KR, Grunfeld C. 2000. The effect of inflammation and infection on lipids and lipoproteins. *In* Feingold KR, Anawalt B, Boyce A, Chrousos G, Dungan K, Grossman A, Hershman JM, Kaltsas G, Koch C, Kopp P, Korbonits M, McLachlan R, Morley JE, New M, Perreault L, Purnell J, Rebar R, Singer F, Trence DL, Vinik A, Wilson DP (ed), Endotext, South Dartmouth (MA).
12. Kaysen GA, Ye X, Raimann JG, Wang Y, Topping A, Usvyat LA, Stuard S, Canaud B, van der Sande FM, Kooman JP, Kotanko P, Monitoring Dialysis Outcomes I. 2018. Lipid levels are inversely

associated with infectious and all-cause mortality: international MONDO study results. J Lipid Res 59:1519-1528.
13. Delekta PC, Shook JC, Lydic TA, Mulks MH, Hammer ND. 2018. *Staphylococcus aureus* utilizes host-derived lipoprotein particles as sources of fatty acids. J Bacteriol 200:(11):e00728-17.
14. Parsons JB, Broussard TC, Bose JL, Rosch JW, Jackson P, Subramanian C, Rock CO. 2014. Identification of a two-component fatty acid kinase responsible for host fatty acid incorporation by *Staphylococcus aureus*. Proc Natl Acad Sci U S A 111:10532-7.
15. Broussard TC, Miller DJ, Jackson P, Nourse A, White SW, Rock CO. 2016. Biochemical roles for conserved residues in the bacterial fatty acid-binding protein family. J Biol Chem 291:6292-303.
16. Cuypers MG, Subramanian C, Gullett JM, Frank MW, White SW, Rock CO. 2019. Acyl-chain selectivity and physiological roles of *Staphylococcus aureus* fatty acid-binding proteins. J Biol Chem 294:38-49.
17. Parsons JB, Frank MW, Jackson P, Subramanian C, Rock CO. 2014. Incorporation of extracellular fatty acids by a fatty acid kinase-dependent pathway in *Staphylococcus aureus*. Mol Microbiol 92:234-45.
18. Hines KM, Alvarado G, Chen X, Gatto C, Pokorny A, Alonzo F, 3rd, Wilkinson BJ, Xu L. 2020. Lipidomic and ultrastructural characterization of the cell envelope of *Staphylococcus aureus* grown in the presence of human serum. mSphere 5(3):e00339-20.
19. Nguyen MT, Hanzelmann D, Hartner T, Peschel A, Gotz F. 2016. Skin-specific unsaturated fatty acids boost the *Staphylococcus aureus* innate immune response. Infect Immun 84:205-15.
20. Bosch M, Sanchez-Alvarez M, Fajardo A, Kapetanovic R, Steiner B, Dutra F, Moreira L, Lopez JA, Campo R, Mari M, Morales-Paytuvi F, Tort O, Gubern A, Templin RM, Curson JEB, Martel N, Catala C, Lozano F, Tebar F, Enrich C, Vazquez J, Del Pozo MA, Sweet MJ, Bozza PT, Gross SP, Parton RG, Pol A. 2020. Mammalian lipid droplets are innate immune hubs integrating cell metabolism and host defense. Science 370(6514):eaay8085.
21. Bae T, Baba T, Hiramatsu K, Schneewind O. 2006. Prophages of *Staphylococcus aureus* Newman and their contribution to virulence. Mol Microbiol 62:1035-47.
22. Arsic B, Zhu Y, Heinrichs DE, McGavin MJ. 2012. Induction of the staphylococcal proteolytic cascade by antimicrobial fatty acids in community acquired methicillin resistant *Staphylococcus aureus*. PLoS One 7:e45952.
23. Tormo-Mas MA, Mir I, Shrestha A, Tallent SM, Campoy S, Lasa I, Barbe J, Novick RP, Christie GE, Penades JR. 2010. Moonlighting bacteriophage proteins derepress staphylococcal pathogenicity islands. Nature 465:779-82.
24. Lee CY, Iandolo JJ. 1985. Mechanism of bacteriophage conversion of lipase activity in *Staphylococcus aureus*. J Bacteriol 164:288-93.
25. Goerke C, Pantucek R, Holtfreter S, Schulte B, Zink M, Grumann D, Broker BM, Doskar J, Wolz C. 2009. Diversity of prophages in dominant *Staphylococcus aureus* clonal lineages. J Bacteriol 191:3462-8.
26. van Wamel WJ, Rooijakkers SH, Ruyken M, van Kessel KP, van Strijp JA. 2006. The innate immune modulators staphylococcal complement inhibitor and chemotaxis inhibitory protein of *Staphylococcus aureus* are located on beta-hemolysin-converting bacteriophages. J Bacteriol 188:1310-5.
27. Tang Y, Nielsen LN, Hvitved A, Haaber JK, Wirtz C, Andersen PS, Larsen J, Wolz C, Ingmer H. 2017. Commercial Biocides Induce Transfer of Prophage Phi13 from Human Strains of *Staphylococcus aureus* to Livestock CC398. Front Microbiol 8:2418.
28. Tran PM, Feiss M, Kinney KJ, Salgado-Pabon W. 2019. phiSa3mw prophage as a molecular regulatory switch of *Staphylococcus aureus* beta-toxin production. J Bacteriol 201:e00766-18.
29. Ubeda C, Maiques E, Knecht E, Lasa I, Novick RP, Penades JR. 2005. Antibiotic-induced SOS response promotes horizontal dissemination of pathogenicity island-encoded virulence factors in staphylococci. Mol Microbiol 56:836-44.

30. Salgado-Pabon W, Herrera A, Vu BG, Stach CS, Merriman JA, Spaulding AR, Schlievert PM. 2014. *Staphylococcus aureus* beta-toxin production is common in strains with the beta-toxin gene inactivated by bacteriophage. J Infect Dis 210:784-92.
31. Goerke C, Wirtz C, Fluckiger U, Wolz C. 2006. Extensive phage dynamics in *Staphylococcus aureus* contributes to adaptation to the human host during infection. Mol Microbiol 61:1673-85.
32. Jung P, Abdelbary MM, Kraushaar B, Fetsch A, Geisel J, Herrmann M, Witte W, Cuny C, Bischoff M. 2017. Impact of bacteriophage Saint3 carriage on the immune evasion capacity and hemolytic potential of *Staphylococcus aureus* CC398. Vet Microbiol 200:46-51.
33. Deutsch DR, Utter B, Verratti KJ, Sichtig H, Tallon LJ, Fischetti VA. 2018. Extra-chromosomal DNA sequencing reveals episomal prophages capable of impacting virulence factor expression in *Staphylococcus aureus*. Front Microbiol 9:1406.
34. Douchet I, De Haas G, Verger R. 2003. Lipase regio- and stereoselectivities toward three enantiomeric pairs of didecanoyl-deoxyamino-O methyl glycerol: a kinetic study by the monomolecular film technique. Chirality 15:220-6.
35. Horchani H, Ben Salem N, Chaari A, Sayari A, Gargouri Y, Verger R. 2010. Staphylococcal lipases stereoselectively hydrolyse the sn-2 position of monomolecular films of diglyceride analogs. Application to sn-2 hydrolysis of triolein. J Colloid Interface Sci 347:301-8.
36. Zheng CJ, Yoo JS, Lee TG, Cho HY, Kim YH, Kim WG. 2005. Fatty acid synthesis is a target for antibacterial activity of unsaturated fatty acids. FEBS Lett 579:5157-62.
37. Cadieux B, Vijayakumaran V, Bernards MA, McGavin MJ, Heinrichs DE. 2014. Role of lipase from community-associated methicillin-resistant *Staphylococcus aureus* strain USA300 in hydrolyzing triglycerides into growth-inhibitory free fatty acids. J Bacteriol 196:4044-56.
38. Kitadokoro K, Tanaka M, Hikima T, Okuno Y, Yamamoto M, Kamitani S. 2020. Crystal structure of pathogenic *Staphylococcus aureus* lipase complex with the anti-obesity drug orlistat. Sci Rep 10:5469.
39. Hammad SM, Pierce JS, Soodavar F, Smith KJ, Al Gadban MM, Rembiesa B, Klein RL, Hannun YA, Bielawski J, Bielawska A. 2010. Blood sphingolipidomics in healthy humans: impact of sample collection methodology. J Lipid Res 51:3074-87.
40. Hanamatsu H, Ohnishi S, Sakai S, Yuyama K, Mitsutake S, Takeda H, Hashino S, Igarashi Y. 2014. Altered levels of serum sphingomyelin and ceramide containing distinct acyl chains in young obese adults. Nutr Diabetes 4:e141.
41. Baek KT, Frees D, Renzoni A, Barras C, Rodriguez N, Manzano C, Kelley WL. 2013. Genetic variation in the *Staphylococcus aureus* 8325 strain lineage revealed by whole-genome sequencing. PLoS One 8:e77122.
42. Kaplan N, Albert M, Awrey D, Bardouniotis E, Berman J, Clarke T, Dorsey M, Hafkin B, Ramnauth J, Romanov V, Schmid MB, Thalakada R, Yethon J, Pauls HW. 2012. Mode of action, in vitro activity, and in vivo efficacy of AFN-1252, a selective antistaphylococcal FabI inhibitor. Antimicrob Agents Chemother 56:5865-74.
43. Airola MV, Shanbhogue P, Shamseddine AA, Guja KE, Senkal CE, Maini R, Bartke N, Wu BX, Obeid LM, Garcia-Diaz M, Hannun YA. 2017. Structure of human nSMase2 reveals an interdomain allosteric activation mechanism for ceramide generation. Proc Natl Acad Sci U S A 114:E5549-E5558.
44. Luberto C, Hassler DF, Signorelli P, Okamoto Y, Sawai H, Boros E, Hazen-Martin DJ, Obeid LM, Hannun YA, Smith GK. 2002. Inhibition of tumor necrosis factor-induced cell death in MCF7 by a novel inhibitor of neutral sphingomyelinase. J Biol Chem 277:41128-39.
45. Astorg P, Bertrais S, Laporte F, Arnault N, Estaquio C, Galan P, Favier A, Hercberg S. 2008. Plasma n-6 and n-3 polyunsaturated fatty acids as biomarkers of their dietary intakes: a cross-sectional study within a cohort of middle-aged French men and women. Eur J Clin Nutr 62:1155-61.
46. Hodson L, Skeaff CM, Fielding BA. 2008. Fatty acid composition of adipose tissue and blood in humans and its use as a biomarker of dietary intake. Prog Lipid Res 47:348-80.

47. Al-Daghri NM, Torretta E, Barbacini P, Asare H, Ricci C, Capitanio D, Guerini FR, Sabico SB, Alokail MS, Clerici M, Gelfi C. 2019. Sphingolipid serum profiling in vitamin D deficient and dyslipidemic obese dimorphic adults. Sci Rep 9:16664.
48. Trinder M, Walley KR, Boyd JH, Brunham LR. 2020. Causal inference for genetically determined levels of high-density lipoprotein cholesterol and risk of infectious disease. Arterioscler Thromb Vasc Biol 40:267-278.
49. Dobner J, Kaser S. 2018. Body mass index and the risk of infection - from underweight to obesity. Clin Microbiol Infect 24:24-28.
50. Lopez MS, Tan IS, Yan D, Kang J, McCreary M, Modrusan Z, Austin CD, Xu M, Brown EJ. 2017. Host-derived fatty acids activate type VII secretion in *Staphylococcus aureus*. Proc Natl Acad Sci U S A 114:11223-11228.
51. Fey PD, Endres JL, Yajjala VK, Widhelm TJ, Boissy RJ, Bose JL, Bayles KW. 2013. A genetic resource for rapid and comprehensive phenotype screening of nonessential *Staphylococcus aureus* genes. mBio 4:e00537-12.
52. Herbert S, Ziebandt AK, Ohlsen K, Schafer T, Hecker M, Albrecht D, Novick R, Gotz F. 2010. Repair of global regulators in *Staphylococcus aureus* 8325 and comparative analysis with other clinical isolates. Infect Immun 78:2877-89.
53. Pathania A, Anba-Mondoloni J, Gominet M, Halpern D, Dairou J, Dupont L, Lamberet G, Trieu-Cuot P, Gloux K, Gruss A. 2021. (p)ppGpp/GTP and malonyl-CoA modulate *Staphylococcus aureus* adaptation to FASII antibiotics and provide a basis for synergistic bi-therapy. mBio 12:e03193-20.
54. Katayama Y, Zhang HZ, Hong D, Chambers HF. 2003. Jumping the barrier to beta-lactam resistance in *Staphylococcus aureus*. J Bacteriol 185:5465-72.

Figure legends

FIG 1 Insertion sites of ϕ13 and ϕ11.1 in *hlb* and *geh* genes, and non-selective cleavage position by Geh activity. (A) Upper, ϕ13 insertion in *hlb*, encoding a sphingomyelinase (Hlb), results in enzyme N-terminal truncation (position 56 aa of the 330 aa protein). Lower, ϕ11.1 insertion in *geh*, encoding a triacylglycerol lipase (Geh) results in enzyme C-terminal truncation (position 643 aa of the 690 aa protein). (B) Geh activity on the triglyceride trilinolein (TNL), position preference and products. Most lipases cleave preferentially at position 1 and liberate mainly 1.2 DG from TNL, whereas Geh cleaves in both positions and can liberate 1.3DG (34, 35).

FIG 2 *S. aureus* lysogenic status impacts incorporation and elongation of C18:2 derived from serum and TNL. (A) The ϕ13 lysogen incorporates more C18:2 from mouse serum than does the non-lysogen. Newman strain (wild type, WT), a ϕ13 lysogen, and an isogenic Δϕ13 derivative were grown 2h in BHI medium containing 10% mouse serum. FAs were extracted and analyzed by gas chromatography. Left, representative FA profiles. The y axis represents relative FA abundance (mV response) at indicated peak positions. FAs in black can be endogenously produced. FAs in purple are not synthesized by *S. aureus* but are incorporated from serum. Right, histograms of relatives amounts of C18:2 incorporated into PLs. Data presented are mean +/- standard deviation (n=4). (B) ϕ13 and ϕ11 lysogeny status impacts C18:2 incorporation from TNL and its elongation. Four isogenic Newman strains (NM), varying in ϕ11.1 and ϕ13 status (21), were grown 2h in BHI medium supplemented with 30 µM TNL (comprising 3 linoleic acid moieties). Left, growth is presented as OD_{600nm} increase in one hour. Middle, total incorporated C18:2 into PLs is determined from peaks of C18:2 and elongated forms C20:2 and C22:2, and expressed in percent of total FAs. Right, C18:2 and its elongated forms are presented as percent of total FA areas, (n=5). p-values were determined by Mann Whitney test on incorporated C18:2 or on C18:2 elongation percentages ((C20:2+C22:2)/(C18:2+C20:2+C22:2)x100). Data presented are mean +/- standard deviation. **, p≤0.01; *, p≤0.05.

FIG 3 C18:2 incorporation from TNL is increased by Geh activity, and mainly due to 1.3DG product. (A) Geh increases incorporation of C18:2 from TNL. USA300 (*geh*$^+$) and the *geh*::tn (SAUSA300_0320) strains, were grown 3h in BHI supplemented with TNL. The Geh inhibitor orlistat (orli; 30 µM) was added as indicated. The *geh*::tn mutant has a C-terminal truncated Geh similar to ϕ11.1 insertion site. Growth and C18:2 incorporation were determined and expressed as in Fig. 1C. Data presented are mean +/- standard deviation (n=3).v p-values were determined by Mann Whitney test on OD/h and on incorporated C18:2. **, p≤0.01; *, p≤0.05. (B) Acylated positions in a diglyceride determine C18:2 incorporation into PLs**.** The four isogenic Newman strains, which differ in ϕ11.1 and ϕ13 prophages (21) were grown 2h in BHI medium supplemented with 10 µM diglycerides comprising two C18:2 moieties; 1,2- or 1.3DG. Relative amounts of incorporated C18:2 determined as in Fig. 1C and presented as FAs issued from 1.2DG or 1.3DG, (n=4). Note that 1.3DG was more efficiently incorporated and more toxic than 1.2DG. Data presented are mean +/- standard deviation.

FIG 4 Plasmid-driven expression of *hlb* limits 1.3DG toxicity in the presence of activated sphingomyelin and increases C16 incorporation in PLs. The USA300 *hlb*$^-$ strains bearing an empty plasmid (p∅) or a plasmid carrying an intact *hlb* (p*hlb*) were grown for 3h in BHI supplemented with 10% mouse serum. 1.3DG (10 µM) was added as C18:2 donor. Activated sphingomyelin (200 µM SM*, see Materials and methods) was added as Hlb substrate. Left, growth is presented as

OD_{600nm} increase in one hour. Right, total C16 incorporated in PLs expressed as percent of total FAs. Data presented are mean +/- standard deviation (n=3). p-values were determined by Mann Whitney test on OD/h and C16 incorporation, *p≤0.05.

FIG 5 *fakB1* and C16 modulate incorporation of 1.3DG-derived C18:2 and its toxicity on growth. USA300 (WT) strain, *fakB1*$^-$, and *fakB2*$^-$ mutants were grown 2 hours in BHI medium supplemented with 10 µM 1.3DG without or with 20 µM C16. (A) Left, FA profiles determined as in Fig. 2A. Purple arrows indicate C18:2 and elongated forms. Right, incorporated C18:2 from 1.3DG determined as in Fig. 2B. (B) Growth is presented as OD_{600nm} per hour. Data presented in histograms are mean +/- standard deviation (n=5). p-values were determined by Mann Whitney test on C18:2 incorporation from 1.3DG and OD/h.**, p≤0.01; *, p≤0.05.

FIG 6 Competition between 1.3DG-derived C18:2 and C16 for FakB1 limits C18:2 incorporation in PLs. RN450 (*fakB1*$^-$) and RN450-R (*fakB1*$^+$) were grown 3h in BHI supplemented with 10 µM 1.3DG without or with 40 µM C16. (A) Left, FA profiles determined as in Fig. 2A. Purple arrows indicate C18:2 and elongated forms. Right, incorporated C18:2 from 1.3DG determined as in Fig. 2B. (B) Growth presented as OD_{600nm} per hour. Data presented in histograms are mean +/- standard deviation (n=5). p-values were determined by Mann Whitney test on C18:2 incorporation from 1.3DG and OD/h.**, p≤0.01.

FIG 7 ϕ13 lysogeny delays *S. aureus* adaptation to anti-FASII AFN-1252. (A) The Newman strain cured for prophages (Δϕ13Δϕ11, presented as Δϕ13) and ϕ13 lysogen (Δϕ11, presented as ϕ13) were grown in 96-well microtiter plates in BHI medium supplemented with 10% mouse serum and 30 µM 1.3DG for C18:2 enrichment. Strains were grown without or with the antibiotic AFN-1252 (0.5µg/ml) which blocks FASII, and without or with GW4869 (50µ M) an Hlb inhibitor. Growth kinetics of anti-FASII adaptation were followed every 20 min by OD_{600} measurements. (B) C18:2 incorporation in the Δϕ13Δϕ11 Newman strain grown in the presence of AFN-1252 (0.5µg/ml), 10% mouse serum and without or with GW4869 (50 µM). Incorporated C18:2 was determined as described in Fig. 1B. Data presented are mean +/- standard deviation (n=4). p-values were determined by the Mann Whitney test on incorporated C18:2; *, p≤0.05.

FIG 8 Model for the roles of ϕ11.1, ϕ13, and *fakB1* as gatekeepers of *S. aureus* phospholipid variability, lipid toxicity, and adaptation to anti-FASII.

(A) ϕ11.1 and ϕ13 prophages prevent activity of Geh and Hlb lipases, and consequent release of FAs that compete for FakB1. According to conditions, these prophages may excise as extrachromosomal episomes, allowing rapid reinsertion and lipase control (33). Three features related to prophage status are presented:
1) ϕ11.1 lysogeny prevents Geh-facilitated release of toxic C18:2 from serum TGs. In the absence of ϕ11.1, or upon stress-induced excision, intact Geh increases C18:2 incorporation. In contrast to other *S. aureus* lipases, Geh can hydrolyze TGs such as TNL at position 2. Release of 1.3DG leads to high incorporation of C18:2 in PLs.
2) 1.3DG-derived C18:2, as produced by Geh when ϕ11.1 is absent, binds to FakB1. FAs are phosphorylated by the fatty acid kinase Fak. FakB1 and FakB2 acyl binding subunits of Fak were initially reported as being specialized in saturated and unsaturated free FA respectively. FAs are then elongated through FASII or directly incorporated in PLs. We show that, in contrast to free

C18:2 or 1.2DG-derived C18:2, 1.3DG-derived C18:2 uses FakB1 for incorporation in PLs; the underlying mechanisms remain to be elucidated.
3) In the absence of ϕ13, or upon stress-induced excision, intact Hlb, together with a ceramidase, lead to C16 release from serum sphingomyelins (SMs). C16 competes for FakB1 binding and is incorporated in PLs whereas the 1.3DG-derived C18:2 is not incorporated. Unbound C18:2 inhibits FASII (32), FA elongation, and bacterial growth.
Consequently, ϕ13 and ϕ11.1 status determines PL composition and *S. aureus* fitness.

(B) Effect of ϕ13 status on *S. aureus* adaptation to an anti-FASII. In serum, *S. aureus* adapts to FASII inhibition using exogenous FAs (6) that are incorporated *via* the Fak system. ϕ13 lysogeny inactivates Hlb and prevents release of saturated FAs such as C16 from serum SMs (see Fig. 8A). FakB1 is then available for 1.3DG-derived C18:2 released from serum TGs. Anti-FASII leads to exogenous FA essentiality and may exacerbate C18:2 toxicity and slow growth. In the absence of ϕ13 or under stress-induced excision, Hlb activity generate FAs that compete with 1.3DG-derived C18:2 for FakB1, protecting membrane and promoting adaptation to anti-FASII. ϕ13 excision during infection (31, 33) may increase bacterial adaptation to anti-FASII.

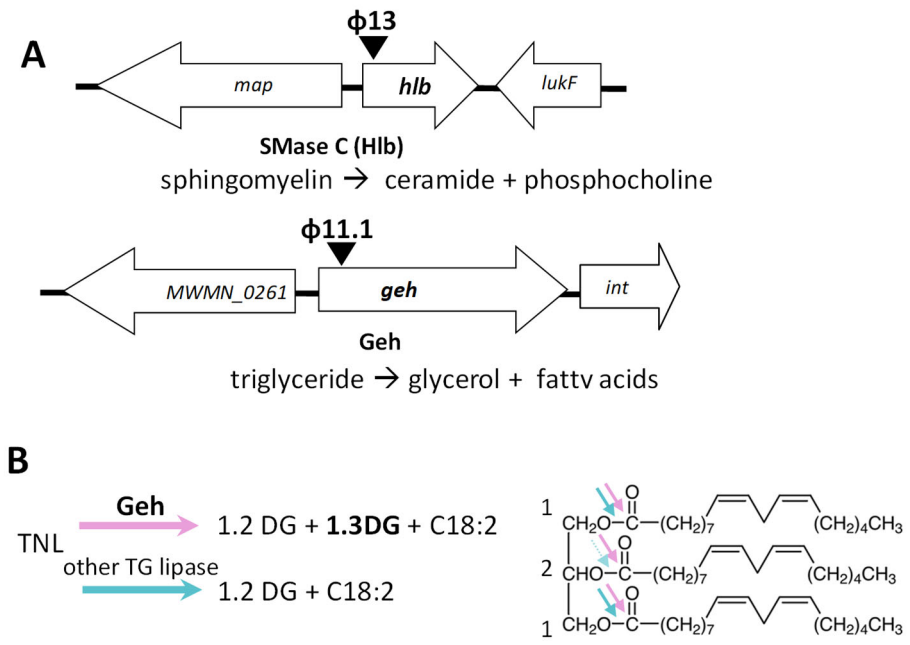
A
ϕ13
map
hlb
lukF
SMase C (Hlb)
sphingomyelin → ceramide + phosphocholine
ϕ11.1
MWMN_0261
geh
int
Geh
triglyceride → glycerol + fattv acids
B
Geh
TNL
1.2 DG + 1.3DG + C18:2
other TG lipase
1.2 DG + C18:2
1
2
1

Fig. 1

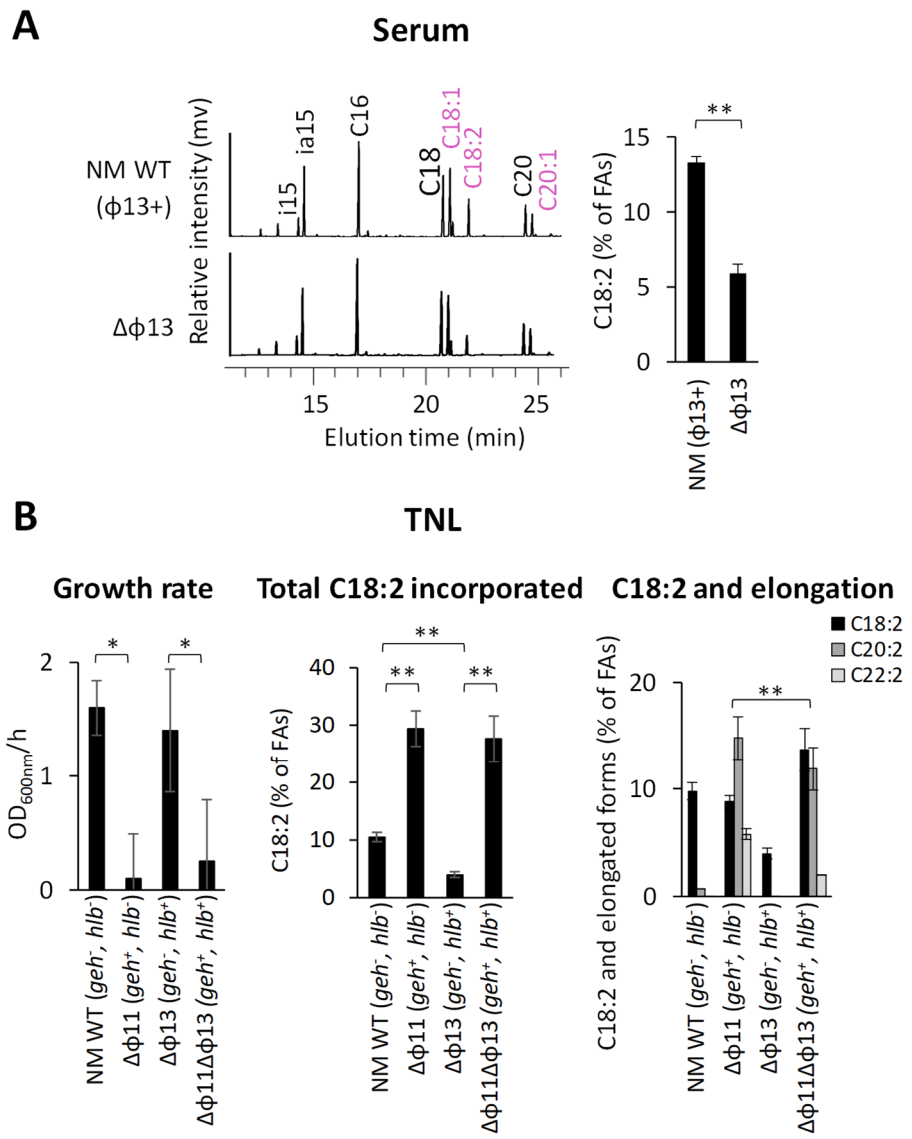
A
Serum
NM WT
(ϕ13+)
Δϕ13
Relative intensity (mv)
i15
ia15
C16
C18
C18:1
C18:2
C20
C20:1
15
20
25
Elution time (min)
C18:2 (% of FAs)
15
10
5
0
**
NM (ϕ13+)
Δϕ13
B
TNL
Growth rate
Total C18:2 incorporated
C18:2 and elongation
OD600nm/h
2
1
0
*
*
NM WT (geh-, hlb-)
Δϕ11 (geh+, hlb-)
Δϕ13 (geh-, hlb+)
Δϕ11Δϕ13 (geh+, hlb+)
C18:2 (% of FAs)
40
30
20
10
0
**
**
**
C18:2
C20:2
C22:2
C18:2 and elongated forms (% of FAs)
20
10
0
**

Fig. 2

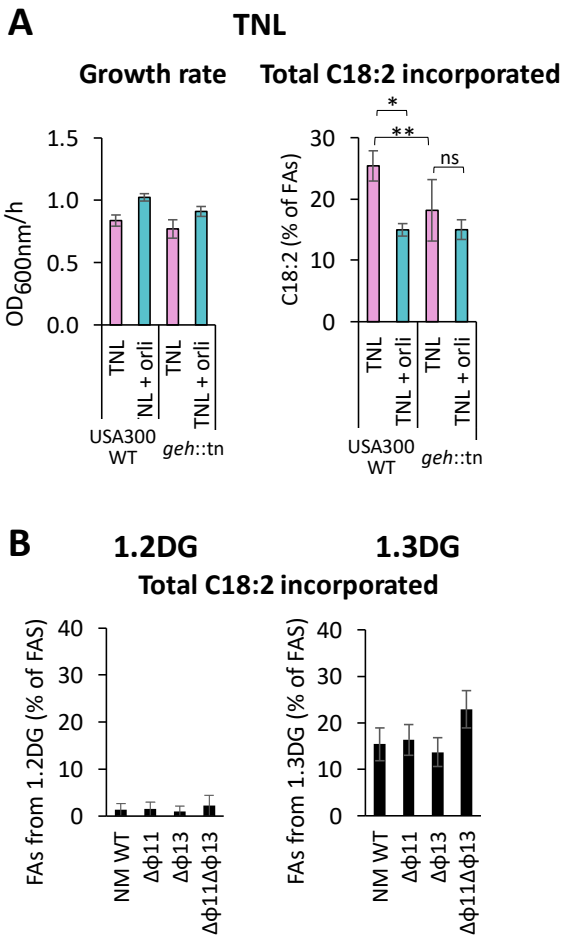
A
TNL
Growth rate
Total C18:2 incorporated
OD600nm/h
1.5
1.0
0.5
0.0
C18:2 (% of FAs)
30
20
10
0
*
**
ns
TNL
TNL + orli
TNL
TNL + orli
USA300 WT
geh::tn
B
1.2DG
1.3DG
Total C18:2 incorporated
FAs from 1.2DG (% of FAS)
FAs from 1.3DG (% of FAS)
40
30
20
10
0
NM WT
Δϕ11
Δϕ13
Δϕ11Δϕ13

Fig. 3

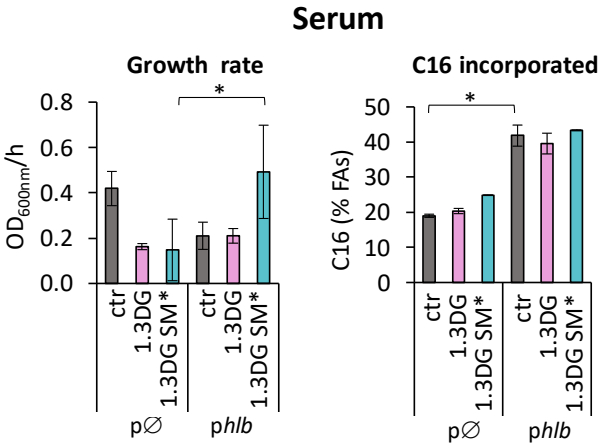
Serum
Growth rate
C16 incorporated
OD600nm/h
C16 (% FAs)
0.8
0.6
0.4
0.2
0.0
50
40
30
20
10
0
*
*
ctr
1.3DG
1.3DG SM*
ctr
1.3DG
1.3DG SM*
p∅
phlb

Fig. 4

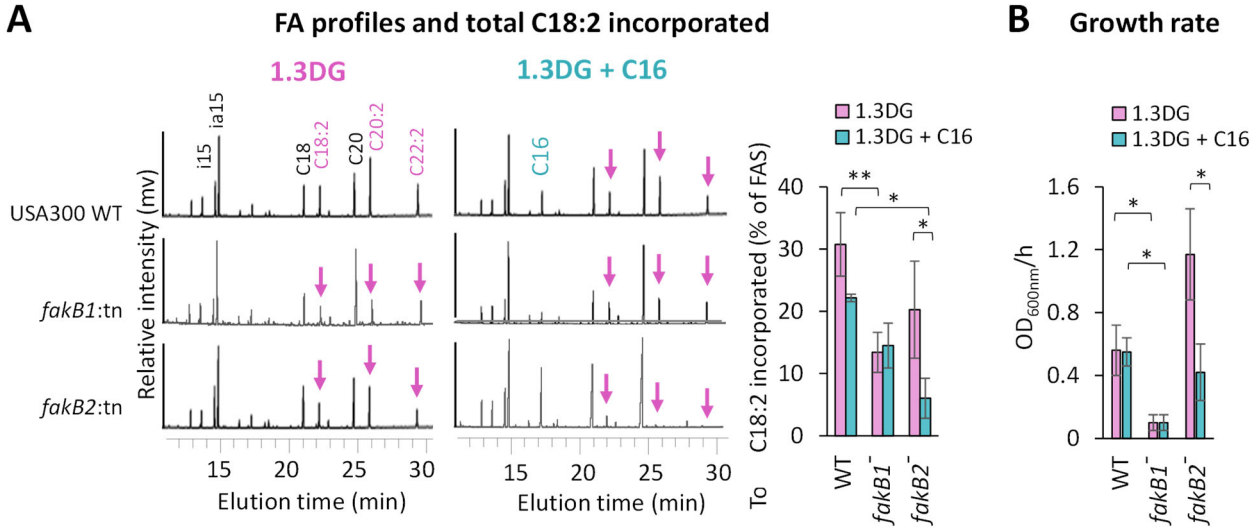
A
FA profiles and total C18:2 incorporated
1.3DG
1.3DG + C16
USA300 WT
fakB1:tn
fakB2:tn
Relative intensity (mv)
i15
ia15
C18
C18:2
C20
C20:2
C22:2
C16
15
20
25
30
Elution time (min)
1.3DG
1.3DG + C16
To C18:2 incorporated (% of FAS)
40
30
20
10
0
**
*
*
WT
fakB1-
fakB2-
B
Growth rate
1.3DG
1.3DG + C16
OD600nm/h
1.6
1.2
0.8
0.4
0
*
*
*
WT
fakB1-
fakB2-

Fig. 5

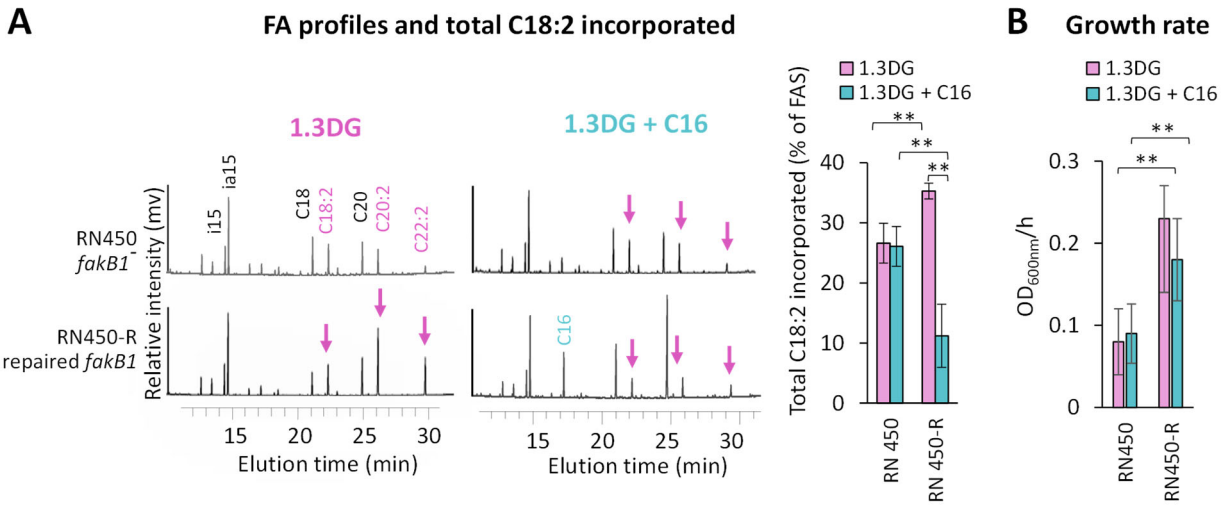
A
FA profiles and total C18:2 incorporated
1.3DG
1.3DG + C16
RN450
fakB1-
RN450-R
repaired fakB1
Relative intensity (mv)
i15
ia15
C18
C18:2
C20
C20:2
C22:2
C16
15
20
25
30
Elution time (min)
Total C18:2 incorporated (% of FAS)
40
30
20
10
0
**
RN 450
RN 450-R
B
Growth rate
OD600nm/h
0.3
0.2
0.1
0
RN450
RN450-R

Fig. 6

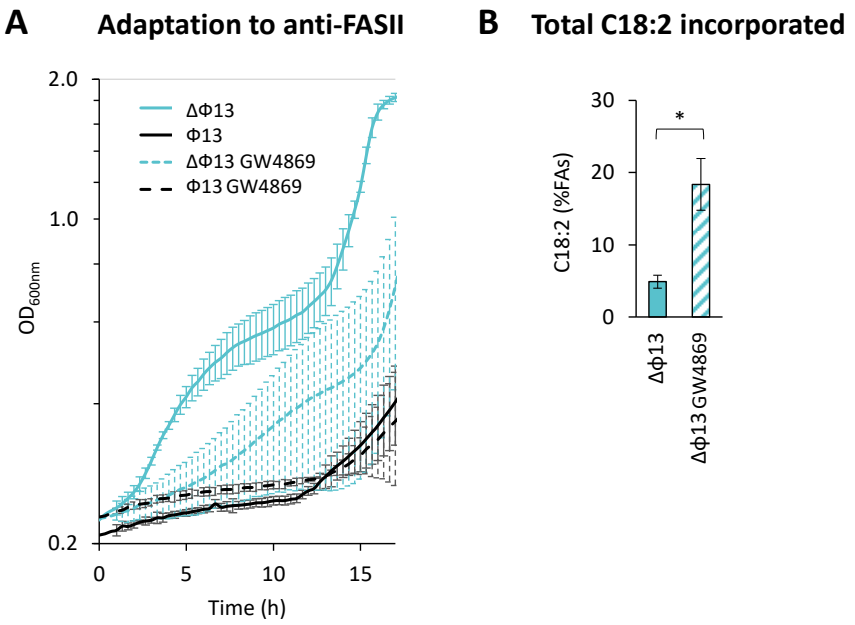
A
Adaptation to anti-FASII
2.0
1.0
0.2
OD600nm
ΔΦ13
Φ13
ΔΦ13 GW4869
Φ13 GW4869
0
5
10
15
Time (h)
B
Total C18:2 incorporated
30
20
10
0
C18:2 (%FAs)
*
Δϕ13
Δϕ13 GW4869

Fig. 7

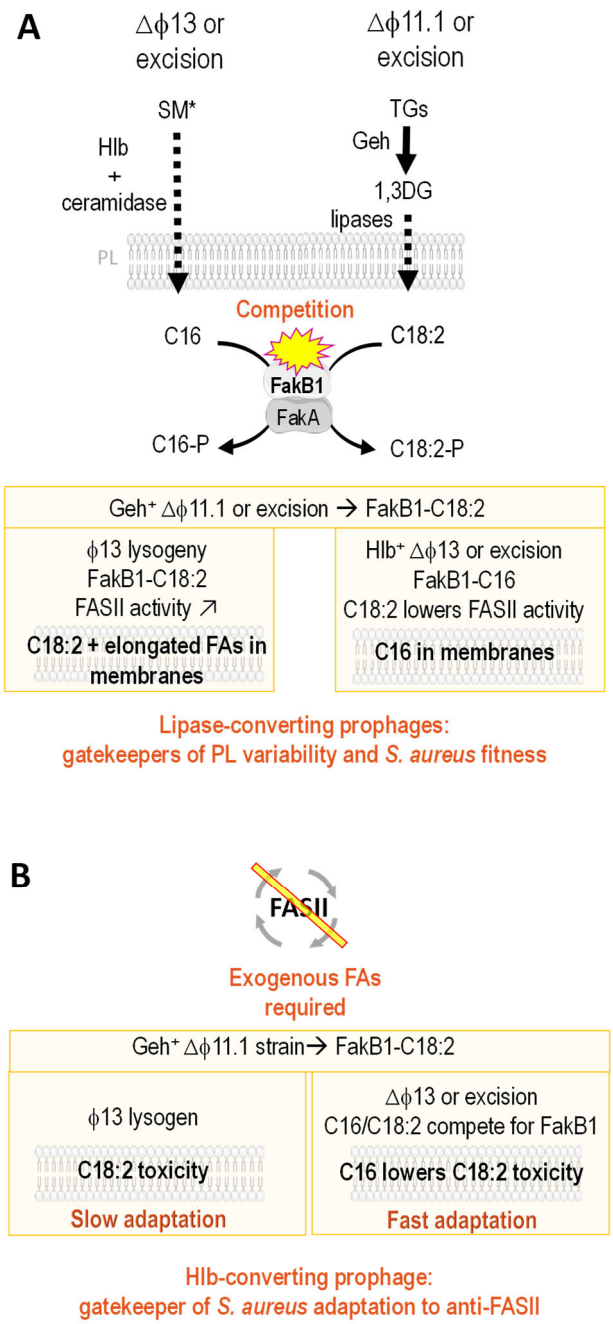
A
Δϕ13 or excision
Δϕ11.1 or excision
SM*
TGs
Hlb + ceramidase
Geh
1,3DG
lipases
PL
Competition
C16
C18:2
FakB1
FakA
C16-P
C18:2-P
Geh⁺ Δϕ11.1 or excision → FakB1-C18:2
ϕ13 lysogeny
FakB1-C18:2
FASII activity ↗
C18:2 + elongated FAs in membranes
Hlb⁺ Δϕ13 or excision
FakB1-C16
C18:2 lowers FASII activity
C16 in membranes
Lipase-converting prophages:
gatekeepers of PL variability and S. aureus fitness
B
FASII
Exogenous FAs required
Geh⁺ Δϕ11.1 strain→ FakB1-C18:2
ϕ13 lysogen
C18:2 toxicity
Slow adaptation
Δϕ13 or excision
C16/C18:2 compete for FakB1
C16 lowers C18:2 toxicity
Fast adaptation
Hlb-converting prophage:
gatekeeper of S. aureus adaptation to anti-FASII

Fig. 8